Journal of Molecular Graphics and Modelling 59 (2015) 50–58

Contents lists available at ScienceDirect

Journal of Molecular Graphics and Modelling

journal homepage: www.elsevier.com/locate/JMGM

Theoretical investigations into the electronic structures and electron transport properties of fluorine and carbonyl end-functionalized quarterthiophenes

Qian Li[a], Yuai Duan[a], Hong-Ze Gao[b], Zhong-Min Su[a,*], Yun Geng[a,*]

[a] Institute of Functional Material Chemistry, Faculty of Chemistry, Northeast Normal University, Changchun 130024, Jilin, People's Republic of China
[b] Fundamental Department, Chinese People's Armed Police Force Academy, Langfang 065000, People's Republic of China

ARTICLE INFO

Article history:
Accepted 3 April 2015
Available online 13 April 2015

Keywords:
Thiophene based transporting material
Fluorination and carbonylation
Electron transport property
Density functional theory

ABSTRACT

In this work, we concentrate on systematic investigation on the fluorination and carbonylation effect on electron transport properties of thiophene-based materials with the aim of seeking and designing electron transport materials. Some relative factors, namely, frontier molecular orbital (FMO), vertical electron affinity (VEA), electron reorganization energy (λ_{ele}), electron transfer integral (t_{ele}), electron drift mobility (μ_{ele}) and band structures have been calculated and discussed based on density functional theory. The results show that the introduction of fluorine atoms and carbonyl group especially for the latter could effectively increase EA and reduce λ_{ele}, which is beneficial to the improvement of electron transport performance. Furthermore, these introductions could also affect the t_{ele} by changing molecular packing manner and distribution of FMO. Finally, according to our calculation, the **3d** system is considered to be a promising electron transport material with small λ_{ele}, high electron transport ability and good ambient stability.

1. Introduction

Organic semiconductor materials have been dramatically developed in the past two decades owing to their potential merits, such as low-cost, large-area coverage, flexibility and ease of processing [1–6]. To achieve more effective and extensive applications, such as organic p-n junctions [7,8], bipolar transistors [9], and organic complementary circuits (CMOS) [10,11], both hole-transporting (p-type) and electron-transporting (n-type) materials are indispensable. However, the development of efficient n-type semiconductors is far behind the p-type's, which is connected to their low electron injection efficiency [12–14] and inferior ambient stability [15–18]. Recently, both experimental and theoretical efforts have proved that introducing strong electron-deficient moieties into traditional p-type materials can change them into n-type ones because of the lower injection barrier and improved molecular stability [19,20].

Thiophene-based transporting materials are a family of preeminent organic semiconductors [21,22] owning to their synthetic availability, widespread possibility and tunable electronic properties [23]. According to the locations of the electron-withdrawing functionalities, such as F, fluorocarbons, CO and CN, the reported n-type thiophene derivatives can be classified into two categories: (i) the ones substituted at the ends of the thiophene chain, that is, bringing in terminal groups; (ii) the ones modified on the side position of the thiophene chain. Thiophene-based materials substituted at the end positions are generally expected to have large π-conjugation by introducing proper aromatic groups, which would provide better intermolecular π···π overlap and thus enhance the transport performance [24–26].

The perfluoroarene and carbonyl terminal modified thiophene-based material **DFCO-4T** is a prominent n-type semiconductor, which exhibits extremely high electron mobility ($\mu_e \approx 0.21\ cm^2\ V^{-1}\ s^{-1}$) [27] in solution-cast film. Fascinated with this, we summarized and analyzed the thiophene-based systems with fluorine or carbonyl group modifications as Fig. 1 shows. It is interesting to note that when a classical p-type thiophene-based transport material is fluorinated by introducing fluoroalkyl, fluorophenyl or fluorine substitutions, the system would always show n-type transport property. While the carbonyl groups do the same. For example, the diperfluorohexyl modified sexithiophene **DFH-6T** exhibits an n-type transport behavior with electron mobility of $0.001\ cm^2\ V^{-1}\ s^{-1}$. [28,29] The **DFH-6T** derivatives with 4 and 5

* Corresponding authors. Tel.: +86 431 85099108; fax: +86 431 85684009.
E-mail addresses: zmsu@nenu.edu.cn (Z.-M. Su), gengyun575@gmail.com (Y. Geng).

http://dx.doi.org/10.1016/j.jmgm.2015.04.001
1093-3263/

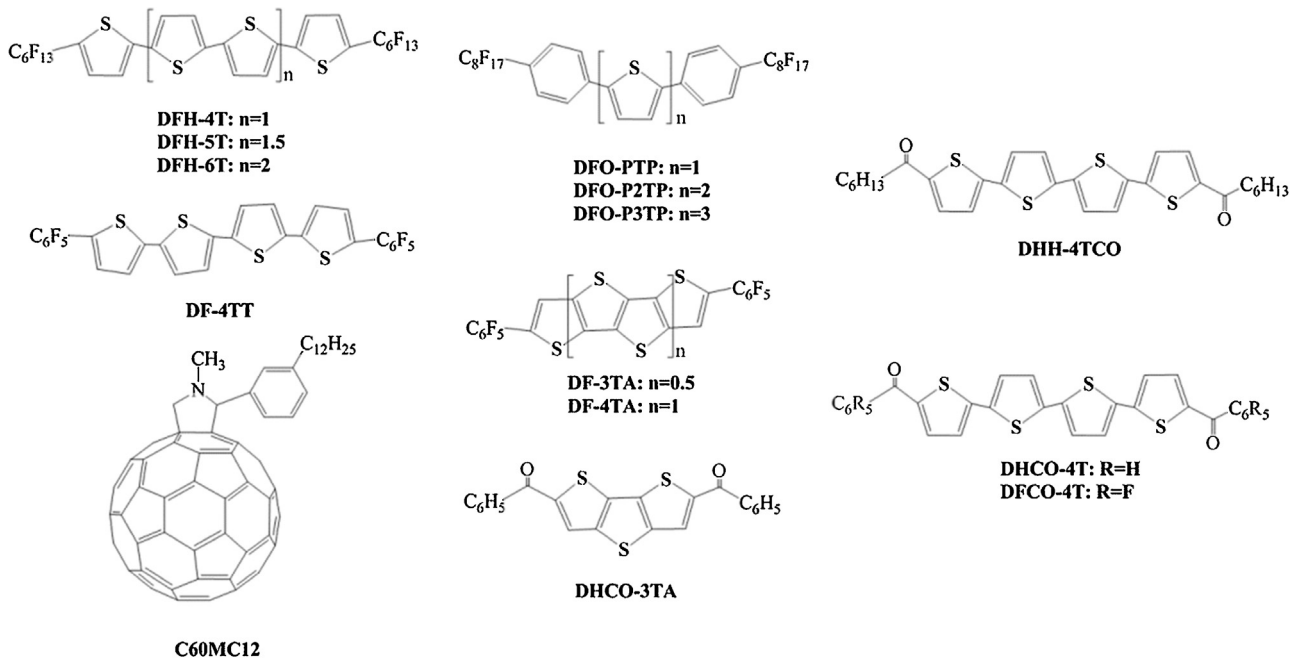

Fig. 1. The reported n-type thiophene-based systems with fluorination and carbonylation along with $\mathbf{C_{60}MC_{12}}$.

thiophene rings [30] and with terminal perfluorooctyl-phenylene modification, such as **DFO-PTP**, **DFO-P2TP** and **DFO-P3TP** [5], also exhibit n-type transport behaviors. Besides, the *F*-substituted systems with other thiophene core conformations also show electron transport behavior, such as iso-quarterthiophene cored **DF-4TT** [21,31], fused-ring thiophene cored **DF-3TA** and **DF-4TA** [32,33]. While, **DHH-4TCO** ($\mu_e \approx 0.1\,cm^2\,V^{-1}\,s^{-1}$) is the only thiophene-based n-type transport material modified by carbonyl groups we can find [34]. Thusly, it is wondered that whether the carbonyl group has any contribution to the electron transport properties in systems like **DFCO-4T** modified with both F atoms and CO group substitutions**,** in what way, and what kind of condition can it happen. It is well-known that the nature of the electron-withdrawing mechanism of the two modifications is different: a $(-I)$ inductive effect is expected for the fluorine substitute, whereas the carbonyl group works as a combination of $(-M)$ π-mediated mesometric and $(-I)$ inductive effects, indicating that the carbonyl group can directly participate in π-conjugation. Does this mean that the CO groups work in a different way with the fluorine substitutes? Here we might say that the mechanism of the carbonyl modification on transport properties is not clear enough, further theoretical study is needed.

What's more, it is reported that comparing to chain linked thiophene cored systems, fused-ring thiophene-cored systems behave flatter molecular structure to ensure better electron delocalization facilitating effective intermolecular overlap, and higher C/H ratio promoting closer π-packing tendency of the system [35]. From this aspect, the conformation of thiophene rings will affect the carrier transport performance. As mentioned above, both fluorine and carbonyl group modifications could convert p-type transport materials into n-type ones. Therefore, we would like to see whether the effects of the substitutions on different conformations of thiophene cores are same. Is the fused-ring thiophene cored systems also exhibit better electron transport behavior after substituted by fluorine or (and) carbonyl group? And which type of thiophene ring conformation is more sensitive to the modifications?

To answer the above questions, we designed the following systems. Three representative thiophene backbones, **1-, 2-** and **3-** series in Fig. 2 were chosen as the investigated subject. In detail: (i) the **1-** series with quarterthiophene (4T) backbone arranging in *trans–trans–trans* conformation; (ii) the **2-** series with quarterthiophene backbone arranging in *cis–trans–cis* conformation; (iii) the **3-** series contain a fused-ring tetrathienoacene. Additionally, the **-a** series are terminal modified with a phenyl group; the **-c** series are the carbonylized systems of **-a** series; and the **-b** and **-d** series are fluorine substituted **-a** and **-c** series, respectively. The electron transport properties of the all 12 systems are systematically investigated with the aim of seeking and designing electron transport materials. Thereby, in this work, some relative factors to transport properties, namely, frontier molecular orbital (FMO), vertical electron affinity (VEA), electron reorganization energy (λ_{ele}), electron transfer integral (t_{ele}), electron drift mobility (μ_{ele}) and band structures have been investigated based on density functional theory calculation. The fluorination and carbonylation effect on electron transport properties was focused on and compared. We hope our study would give a hint for experimental research.

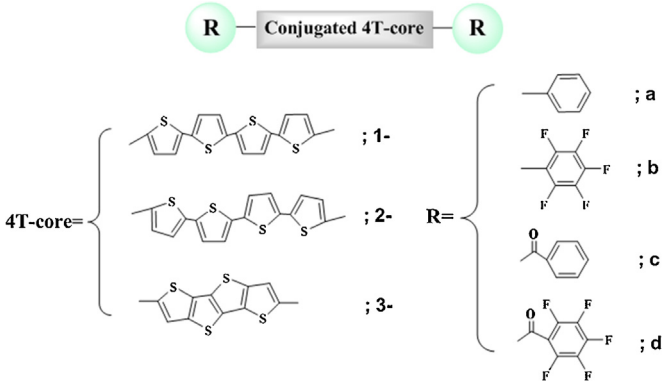

Fig. 2. The molecular model of the systems investigated here with 4T-cores named by numbers (**1**, **2**, **3**) and terminal modifications named by letters (**a**, **b**, **c**).

2. Theoretical and computational methodology

To optimize molecular geometry, both B3LYP [36,37,38] and B3P86 [39,40] functionals with 6-31G(d,p) [41–43] and 6-31+G(d,p) [44,45] basis sets were employed in Gaussian 09

program package [46]. Then, the ONIOM [47] (QM:MM) [48] method was applied using Universal Force Field (UFF) to consider the intermolecular packing effect on the geometrical structure. Besides, the studied systems were also optimized by fixing main torsional dihedral angles to shorten the error in optimized dihedral angles.

The AOMIX program [49] was used to give a quantificational analysis on the contributions of different fragments to the electronic distribution of frontier molecular orbitals (FMOs). All compounds were separated into three fragments: the 4T-core, the terminal phenyl or perfluorphenyl groups and the carbonyl modifications.

Generally speaking, there are two mainly mechanisms describing charge transport in organic crystal semiconductors: (i) the coherent band model, and (ii) the incoherent hopping model. For the former, the carriers are delocalized and perform coherent transport feature, besides, the mobility would decrease with increasing temperature. While for the latter, the carriers inspired by thermal energy hop incoherently between adjacent sites, and contrary to the former, the mobility increases with temperature. However, the band theory or its extensions are generally employed for perfectly ordered defect-free organic crystals at low temperature. Here we defined the calculated temperature as 300 K, where the charge could be strongly localized and the lattice phonons are closely coupled with the charge motion, suggesting the hopping mechanism's superiority [19,50]. Thusly, the hopping mechanism was adopted in this work.

According to hopping mechanism, the charge-transport (CT) rate between two adjacent molecular sites i and j is given in classical Marcus formulation [51].

$$k = t^2 \left(\frac{\pi}{h^2 k_B T \lambda}\right)^{1/2} \exp\left(\frac{-\lambda}{4 k_B T}\right) \tag{1}$$

where t represents charge transfer integral between molecular site i and j, h is the Planck constant, k_B is the Boltzmann constant, and T is the temperature as mentioned above, which is defined as 300 K, λ represents the reorganization energy.

Since all other parameters are constants, as the formulation reveal, two main parameters determine the charge-transport (CT) rate: the reorganization energy (λ) and the intermolecular transfer integral (t).

For the reorganization energy (λ), it consists of contributions from the inner reorganization energy λ_{in} and the external polarization energy λ_{out} [52–54] which is excluded here due to the negligible contribution [47]. The inner reorganization energy λ_{in} can be evaluated either from the adiabatic potential-energy surfaces [55] or the normal-mode (NM) analysis [25]. In this paper, we use the former, in which the λ_{in} can be seemed as a sum of two relaxation energies, i.e.,

$$\lambda_{in} = \lambda_{rel}^{(1)} + \lambda_{rel}^{(2)} = \left[E^0\left(g^c\right) - E^0\left(g^0\right)\right] + \left[E^c\left(g^0\right) - E^c\left(g^c\right)\right] \tag{2}$$

Respectively, $E^0(g^0)$ and $E^c(g^0)$ are the energies in the neutral and charged states under the optimized geometry of the neutral species; Similarly, $E^0(g^c)$ and $E^c(g^c)$ are the energies in the neutral and charged states under the optimized geometry of the charged species.

For the intermolecular transfer integral, several methods have proved to successfully evaluate it, e.g., the minimized energy level splitting along the reaction path method [56], the direct evaluation method [57] and the site-energy corrected coupling method [58]. In this work, we chose site-energy corrected method and calculated the transfer integrals at PW91PW91/6–31G(d,p) level. For the site corrected method, the transfer integral (t) can be expressed by:

$$t_{ij}^{\text{eff}} = \frac{\left[t_{ij} - \left(1/2\right)\left(t_i + t_j\right)S\right]}{\left(1 - S^2\right)} \tag{3}$$

here $t_i = \langle \Phi_i | H | \Phi_i \rangle$, $t_j = \langle \Phi_j | H | \Phi_j \rangle$ and $t_{ij} = \langle \Phi_i | H | \Phi_j \rangle$. Wherein, the Φ_i and Φ_j represent the HOMOs (or LUMOs) of the adjacent molecules i and j for the hole transport (electron transport). H and S are the dimer Hamiltonian and the overlap integral between the monomer HOMOs (or LUMOs), respectively.

As a connection of experimental and theoretical results, under the fixed temperature, the drift mobility μ can be calculated from Einstein–Smoluchowski relation:

$$\mu = \frac{eD}{k_B T} \tag{4}$$

where e is the electronic charge, and D is the diffusion coefficient, which can be approximately expressed as [59,60]:

$$D = \frac{1}{2n\Sigma_i d_i^2 k_i P_i} \tag{5}$$

here i represents a specific hopping pathway with r_i being the electron hopping centroid-to-centroid distance; d is the spatial dimension. While $P_i = k_i/\Sigma k_i$ is the relative probability for electron hopping to the ith neighbor.

Meanwhile, to understand the carrier transport behavior from another aspect we calculated the band structures of the systems **1d**, **2b**, **3a** and **3b** with VASP [61,62,63] using the PBE (Perdew–Burke–Ernzerhof) exchange–correlation functional [64] and a plane-wave basis set, the integrations over the Brillouin zone were, respectively, sampled by $1 \times 7 \times 8$, $5 \times 4 \times 3$, $7 \times 5 \times 1$ and $1 \times 6 \times 2$ for systems **1d**, **2b**, **3a** and **3b**, using the Monkhorst–Pack scheme [65]. All the k points were tested through estimating the convergence of the surface energy before we calculated the bands, and finally we selected the number of k-points for each system as described above, which can strike a balance between calculation accuracy and efficiency.

3. Result and discussion

3.1. Geometric optimization strategies

The systems **1c**, **1d**, **2b**, **3a** and **3b** were fully optimized using different DFT methods B3LYP/6-31G(d,p), B3P86/6-31G(d,p) and B3P86/6-31 + G(d,p). The HOMO–LUMO energy gaps of all systems were calculated based on the optimized structures and compared with the experimental results (see Fig. S1). Simultaneously, all the optimized structures were also compared with the available crystal structures (see Fig. S2). According to Fig. S1, the B3P86/6-31G(d,p) method give a better prediction concerning the HOMO–LUMO energy gaps, which follow the same trend with the experimental results, although the highest derivation between experimental and theoretical values reaches about 0.2 eV (for **1b**). The experimental HOMO–LUMO energy gaps were estimated from the onset of the optical absorption in solvent [27,31,33], whereas we calculated these values based on bond theory for single molecule. A slight deviation between experimental and theoretical values is considered to be rational. As shown in Fig. S2, both B3P86/6-31 + G(d,p) and B3P86/6-31G(d,p) methods give very good structures agreeing with the experimental ones in terms of both bond lengths and bond angles. The deviations between computational and experimental results are within 0.03 Å and 5.0°. While the results derived from B3LYP/6-31G(d,p) method are not as accurate as the ones obtained by B3P86 methods. Considering both the HOMO–LUMO energy gap and the molecular geometry, the B3P86/6-31G(d,p) method was

chosen as the fundamental optimization method. It should be noted that some dihedral angles (see Fig. S5) of the calculated systems were misvalued by 10–25 °for both B3LYP and B3P86 methods. These errors could be caused by ignoring the packing effect of surrounding molecules in the crystals.

To accurately evaluate molecular geometries of systems studied here, we further considered the influence of surrounding molecules in two ways. First a packing model of systems **1c**, **1d**, **2b**, **3a** and **3b** were selected from X-ray structures in following way as shown in Fig. S4, namely, the molecular cluster shell was retained surrounding the center molecule for each system. Then the QM/MM (B3P86:UFF) method was employed to optimize their geometries. The results, as Fig. S2 shows, exhibit a better coherence with the corresponding experimental data than the ones by directly optimizing single molecule in gas phase, especially for the dihedral angles. In this case, the deviations of the calculated systems from the experimental ones fall down to tolerable degree of 3–14°. Since the main variations happened in some main inter-ring torsions, we simplified the process to optimize the systems, **1c**, **1d**, **2b**, **3a** and **3b**, which are the systems with crystal structures, by fixing the inter-ring dihedrals at their corresponding experimental values (see Fig. S5). As Fig. S2 shows, this method maintains the accuracy of both bond lengths and bond angles predictions. For the other systems, we performed analogous geometry optimization, concretely speaking, the dihedral angles on the cores of **1-** and **2-** series were fixed, and the torsions between the cores and the terminal modifications of **3-** series were also fixed.

Besides, as previous study of our group explicate [66], simply optimizing the molecule in gas-phase would overestimate the molecular geometric variation from neutral state to ionic states, as a result the reorganization energy, which is one of the key parameters affecting the carrier transporting behavior as Marcus formula supposed, would be overestimated.

3.2. Frontier molecular orbital

The energy levels of FMO are key parameters for assessing the carrier injection ability and stability of the material. Generally speaking, the high HOMO and low LUMO energy levels, respectively, ensure efficient hole and electron injections [67], and lower FMO energies always ensure higher ambient stability [23]. Besides, the distribution of FMO will affect the intermolecular orbital overlap integral (t_{ij}) of a dimer, and thusly influence the t as Eq. (3). In this section, we will discuss how the FMO energies and their distributions are affected by fluorine and carbonyl group modifications.

Fig. 3 shows the FMO energies and HOMO–LUMO energy gaps of the studied systems. According to this figure, we not only prove again the view that introducing strong electron-withdraw groups could lower the FMO energy level as previous studies mentioned [25], but also drawn some novel conclusions based on this work as follows: (i) Comparing the **-b** with **-c** series, we could find that the carbonyl group substituted thiophene-based systems have lower LUMO energy levels than the fluorine substituted ones. In addition, the **-d** series substituted by both carbonyl groups and fluorines exhibit the lowest LUMO energy levels, but the degree of the fall in energy level was not a simple summation of them. (ii) When fluorine or carbonyl group is introduced in **3-** systems, the fall in energy level is more significant than those of the **1-** or **2-** systems. This phenomenon may be attributed to the better conjugation and flatter molecule structure of **3-** systems; (iii) The **3-** series have the largest HOMO–LUMO energy gaps, no matter whether adding any electron-withdraw modifications or not. Besides, the **3d** system could be a promising electron transporting material since it exhibits the lowest LUMO energy level and FMO energies.

The distributions of FMOs of all systems are depicted in Fig. S6. According to the figure, we can see that the electron density

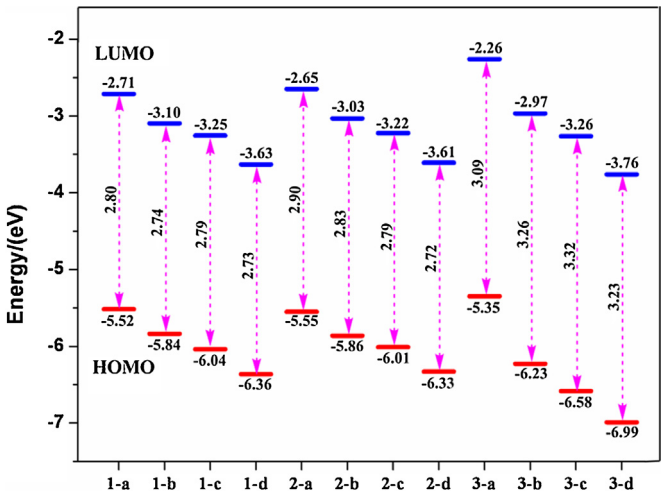

Fig. 3. The HOMO and LUMO energy levels for the neutral states of all systems. Energy gaps are listed between the HOMO and LUMO energy levels.

distribution on F atoms is little, while there is quite much density distribution on O atoms of the carbonyl groups in FMOs, as the carbonyl group can directly participate in π-conjugation, that is, it exhibits conjugative effect. As a result, the effect of lowing in FMO energy is more evident for carbonyl groups. What's more, it is concluded from Fig. S6 that the carbonyl groups can affect the distributions of FMOs to an extent. In addition, by comparing the fluorinated **-b** and **-d** series, it was found that the FMO distributions on F substitutes were further eliminated by carbonyl groups. What's more, the conjunctions are cut off by introducing hexatomic-ring modifications on the terminal position of thiophene cores, leading to the FMOs mainly locating at the remaining 4-thiophene-ring frameworks, which means the conformation of 4-thiophene-ring backbone is critical for manipulating the energy gaps of the systems, since the length of conjunction chain is known to be negative correlation with energy gap. That is why the HOMO–LUMO energy gap of **3-** series is the largest, because they have the shortest conjugated backbone.

A quantificational analysis was carried out by AOMIX program. According to Fig. 4, some conclusions were drawn by comparing the FMO distributions on three divided fragments of the systems, namely, the center thiophenes core, the terminal phenyl or perfluorphenyl groups and the modified carbonyl groups. First, by comparing the LUMO and HOMO distributions, we could see that both the electrons of HOMOs and LUMOs mainly distribute on the thiophene-core backbones. The terminal hexatomic-rings and carbonyl groups make more contributions to the LUMOs than HOMOs. Second, for the effects of introducing fluorine substitutions, there are two situations: for the series **-a** and **-b**, there are more electron distributions of LUMOs on the terminal phenyl for fluorine substituted systems (**-b** series) than the unsubstituted ones (**-a** series). For instance, the distribution of LUMOs on the terminal phenyl of systems **1a**, **2a** and **3a** are 12%, 13% and 28%, respectively, while for the fluorine substituted ones, these parts occupy more LUMO reaching to 17%, 18% and 34% for systems **1b**, **2b** and **3b**. When the carbonyl substituted series **-c** and **-d** are compared, some conclusions were drawn as follows: (i) For systems **1c** and **1d**, the substitution of F atoms makes the LUMO distributions on **4T** trunk slightly increase by 4%. (ii) For systems **2c** and **2d**, the LUMO distributions on both **4T** trunks and the terminal hexatomic rings decrease slightly with substituting F atoms. (iii) While for systems **3c** and **3d**, the LUMO distributions on **4T** trunk heavily decreases by 27%, and the ones on terminal hexatomic rings increase by 14% and the ones on carbonyl groups increase by 13%. Third, for the effects of introducing

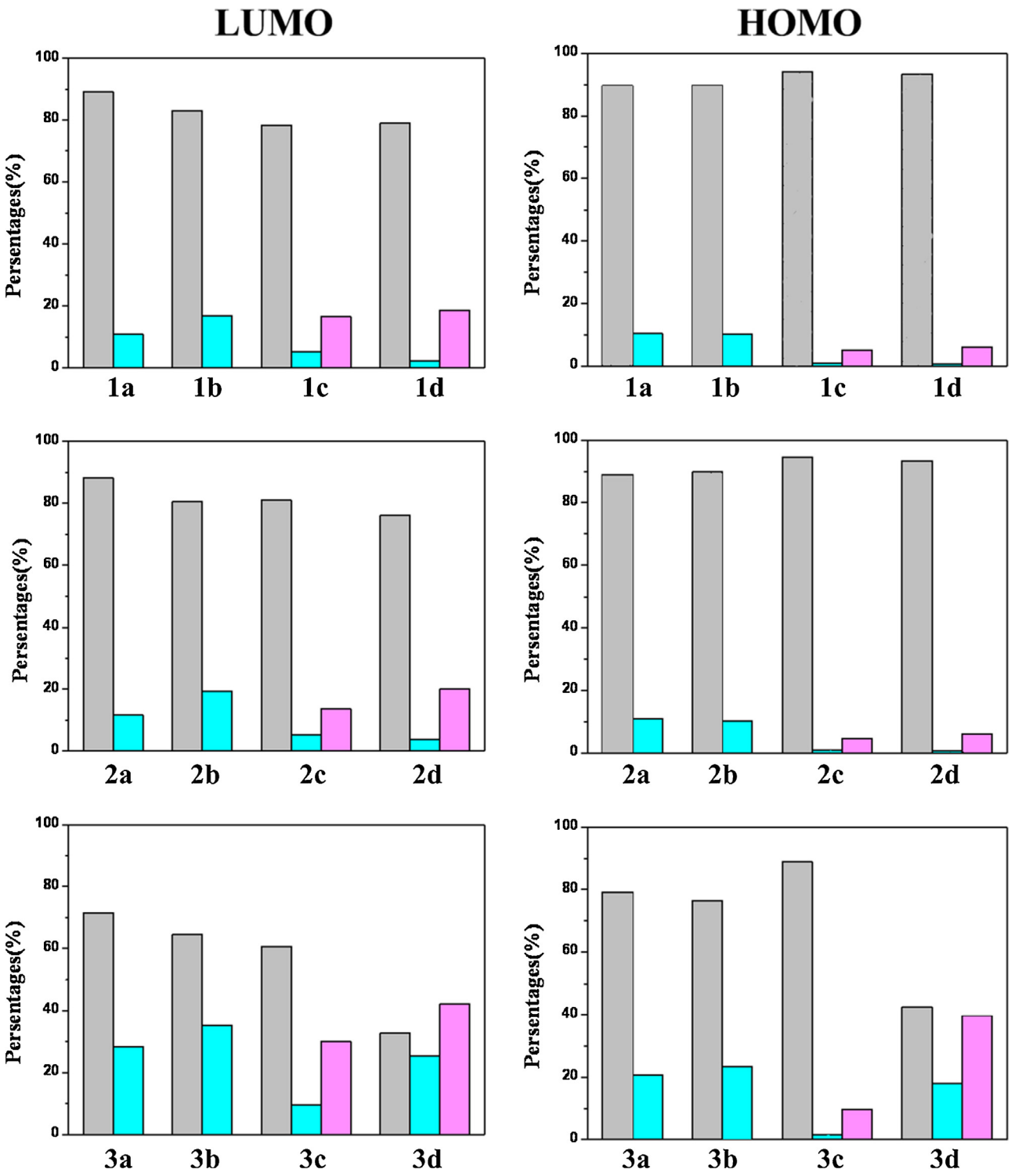

Fig. 4. The distributions of LUMOs and HOMOs of all the systems. Respectively, the gray columns represent the 4T-cores, the cyan columns represent the terminal phenyl or perfluorphenyl groups, and the pink columns represent the modified carbonyl groups. (For interpretation of the references to color in this figure legend, the reader is referred to the web version of this article.)

carbonyl groups, by comparing the **-a** with **-c** series and **-b** with **-d** series, respectively, we proposed two rules here. One is that, there are more contributions from carbonyl groups to FMOs than the ones from the terminal (perfluor)phenyls, and the introduction of carbonyl groups further decrease the FMO distribution on (perfluoro)phenyl groups. Another is that, the LUMO distributions on **4T** backbones are depressed by introducing carbonyl groups, while the HOMO distributions on **4T** backbones are increased. Except for the **3d** system, in which both LUMO and HOMO distributions on thiophene-core backbones are decreased after carbonylation. In a word, the distribution of FMOs are affected by fluorination and carbonylation, this may affect the overlap integral S in dimers and so as the transfer integral t, which will be further discussed in Section 3.4.

3.3. Electron affinity and electron reorganization energy

The electron affinity (EA) is defined as the amount of energy changed when an electron is added to a neutral atom (vertical electron affinity) or deprived of a negative ion (adiabatic electron affinity) [68]. For electron transport materials, a molecule with high EA could trap electron easily, which would benefit the injection process from electrode to the material. And as the Marcus formula supposed, the smaller the λ_{ele} is, the better electron transport performance will be. Here both the vertical electron affinities (VEA) and λ_{ele} were calculated.

Fig. 5 shows the VEA and λ_{ele} of all systems. According to Fig. 5, the VEA increases in the order of introducing —F, —CO, and both the —F and —CO for the series **-b**, **-c** and **-d**, respectively, with the identical thiophene cores. Besides, the VEA values of the systems with the same modification follow the trends **1-** > **2-** > **3-**.

The electron reorganization energy was analyzed for its importance to the electron transport performance. According to Fig. 5, introducing electron-withdrawing groups can to some extent lower the value of λ_{ele} for **2-** and **3-** series. For **2-** series, comparing to the unmodified **2a** system, the reductions of λ_{ele} are 9%, 24% and 20% for **2b**, **2c** and **2d** systems, respectively. And for **3-** series, the percentages of decrease in λ_{ele} are 20%, 14% and 13%, respectively, for **3b**, **3c** and **3d** systems comparing to the **3a** system. While for **1-** series, the λ_{ele} of **1b**, **1c** and **1d** decreases by 7%, 1% and 6%, respectively, comparing to the **1a** system.

In conclusion, by introducing —F or (and) —CO modifications to a system, the VEA can be heightened, meanwhile the decrease of λ_{ele} (or at least keep at the same level) leads to better electron transport performance. So we supposed that the **-d** systems should be excellent electron transporting materials. And we also concluded the reorganization energy derived from gas phase optimization with and whithout fixing dihedral angels, as Table S1 shows, as expected, all the former are lower than the later about 10 meV.

3.4. Electron transfer integral, electrostatic potentials and electron drift mobility

As the Marcus formula supposed, the transfer integral (t) is another vital factor determining the electron mobility except for reorganization energy. The intermolecular orbital overlap integral (S) is a significant factor determining t. In dimers, S is the product of the HOMOs' (LUMOs') coefficients of the monomers, hence the value of S is affected by two aspects. One is the FMO distribution of monomers, and the delocalization and phase of FMO is closely correlated to S. To achieve high t_{ele}, the LUMO should be as delocalized as possible. Another is the packing motif of the dimer, and a transport path with face-to-face π stacking manner will maximize the effective FMO overlap, and thusly achieve highest t [69]. While, due to the electrostatic repulsion, it is hard to form close intermolecular π···π packing path in crystals. An alternative packing manner is herringbone in which the molecules follow side-to-face packing sequence driven by C—H···π intermolecular intereaction. The herringbone packing path also exhibits good t owing to short intermolecular distance ensuring effective FMO overlap. In all, to achieve high charge transport ability, predicting and manipulating the packing manner of transport materials are becoming top issues.

The absolute electron transfer integral values (t_{ele}) and the main transport paths (Here, only the value of t_{ele} larger than 1 meV were taken into account) of systems **1c**, **1d**, **2b**, **3a** and **3b** are shown in Fig. 6. As said above, the highest t is always calculated along face-to-face π-stacking direction, commonly, the larger overlap interaction area of the dimer is, the bigger transfer integral value is. Here, path 1 in **1d** and **3b**, the path 2 in **1c** and path 4 in **2b** are along the π stacking directions with biggest t_{ele} values. Especially, the t_{ele} value of path 1 in **3b** is extremely large, as the overlap interaction area of the dimer in the path is quite large. While, for **3a**, the path 1 and path 2 with C-H. . .π packing exhibit larger t_{ele} values than the path 3 with π stacking, and as a matter of fact, the overlap in the path 3 with π stacking of **3a** just cover a small area.

The fluorinated systems **1d**, **2b** and **3b** exhibit electron transport behaviors when they were applied in OFET devices. It should be noted that the **1c** system exhibits relative high EA, small λ_{ele} and fine t_{ele} values, from this, we could consider that in a certain condition the **1c** system might exhibits electron transport performance. Finally as Fig. 6 shows, most systems like **1c**, **1d**, **3a** and **3b** show 2-D transport behavior, except for **2b** system, which shows 3-D transport behavior.

To probe the effects of fluorine and carbonyl groups substitution on the packing manners of materials, the calculation of electrostatic potential (ESPs) distributions of the systems was carried out. It is reported that the molecular packing manner in a crystal is mainly driven by intermolecular electrostatic interaction [25], and the distribution of ESP in monomer can explain a packing manner to an extent. Therefore, it is naturally concluded that if introducing fluorine (or) and carbonyl groups varies the ESP distribution,

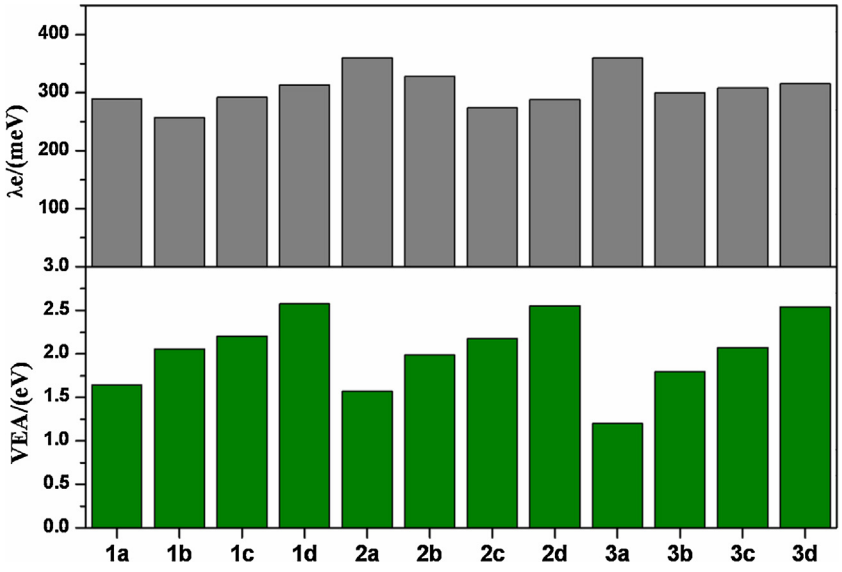

Fig. 5. The vertical electron affinities and electron reorganization energies of all systems.

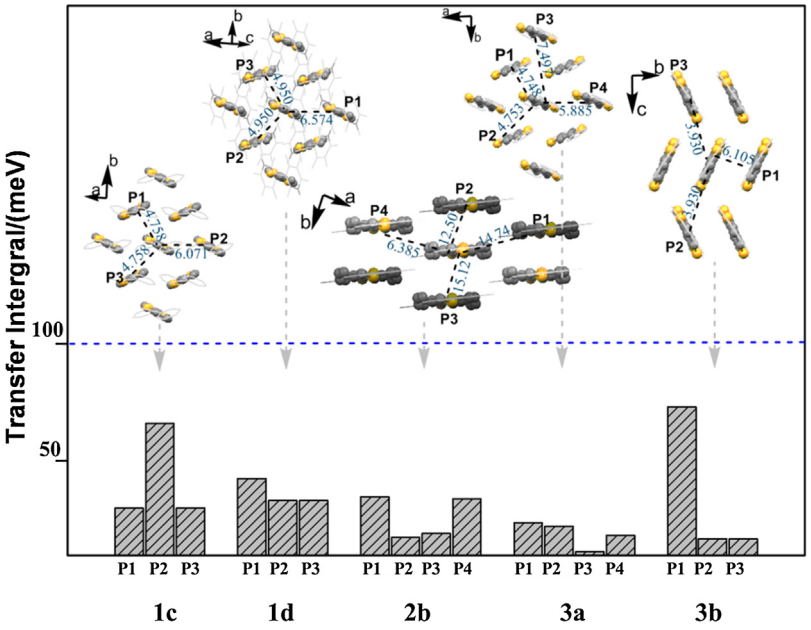

Fig. 6. Absolute electron transfer integral values and the main paths of systems **1c**, **1d**, **2b**, **3a** and **3b**. The centriod-to-centriod distance of each path is also marked in blue. (For interpretation of the references to color in this figure legend, the reader is referred to the web version of this article.)

the packing manner of the material would be probably changed. According to Fig. S7, we found the following rules. First, it was concluded that the carbonylation can dramatically regulate the distribution of ESP of the systems, by comparing the **-a** with **-c** and **-b** with **-d** series, respectively. Second, based on whether the system with or without carbonyl groups, two situations were separated to illustrate the effects of fluorination. For systems without carbonyl groups, there are significant changes on the ESP distribution of series **-a** and **-b**. And for systems with carbonyl group, the series **-c** and **-d** exhibit basically the same ESP distribution. Besides, introducing carbonyl group will form a negative charged center on the O atoms. It appers that carbonyl group contributes more to the ESP distribution than fluorine substitute. In conclusion, substituting fluorine and carbonyl groups will affect the distribution of ESP, especially for the latter, as a result, the packing manner will be varied and so as the carrier transport performance.

The mobilities of systems **1d**, **2b** and **3b** were evaluated using Marcus formalism. According to Table 1, the μ_{ele} of the three systems were all underestimated, especially for system **1d**. The calculated μ_{ele} of system **1d** was 0.05 $cm^2 V^{-1} s^{-1}$, while the experimental value is 0.51 $cm^2 V^{-1} s^{-1}$. We consider that the Marcus–Levich–Jortner formulation should give a better result and the further study is under process.

3.5. Band structure

The band structures of systems **1d**, **2b**, **3a** and **3b** were calculated to give a further understanding on the electron transport behaviors from another perspective. In **1d** and **3b** systems, there are two inequivalent molecules in the primitive unit cells, and as a result, there appeared two subbands in both the valence band (VB) and conduction band (CB). **3a** system has four inequivalent molecules in the primitive unit cell, thusly the VB and CB consist of four subbands.

According to band theory, larger conduction bandwidth signifies better electron transport behavior [26]. Table 2 summarizes the conduction bandwidths (CBW) and band gaps of systems **1d**, **2b**, **3a** and **3b**. Regrettably, the calculated band gaps on the basis of crystal structures are all much underestimated compared to the experimental results. Based on two reasons as follows, the calculations for band gap were considered to be successful to some extent. First, the experimental results are derived from optical stimulated values, which may be affected by many external factors, such as temperature, solvent, atmosphere pressure, etc. Second, it is widely accepted that density functional theory underestimates the band gaps, and our results also proved this point. In Ref. [26] of our manuscript, the band structure of the same system **2b** was also calculated with a DFT functional (with DND basic set). The band gap of system **2b** was 1.44 eV in that study, which is in accordance with ours 1.52 eV. It was obvious that the **3a** system, which is the only p-type transport material among them, displays the smallest CBW. What's more, the CBWs of the other three systems follow the trend of **3b** > **1d** > ≈**2b**. Considering the anisotropy of carrier transporting process, the subzone dispersions in CBs should be further investigated.

It was confirmed that the directions with larger dispersions are all along the paths with bigger transfer integrals [35]. As shown in Fig. S8, in system **1d**, there are two strongest CB dispersions

Table 1
The electron drift mobilities (given by $cm^2 V^{-1} s^{-1}$) of systems **1d**, **2b** and **3b**. The molecular geometries were optimized in both gas phase (up titled by *) and under fixed main torsions.

Systems	μ^* (3-D)	μ (3-D)	μ^{expt}
1d	0.04	0.05	0.51
2b	0.12	0.15	0.43
3b	0.11	0.12	0.30

Table 2
Conduction bandwidths and band gaps derived from the crystal structures of **1d**, **2b**, **3a** and **3b** systems. And the experimental Energy gaps (superscript by exp) were all derived from optically testing in hexafluorophosphate/THF solvent at room temperature.

Systems	CBWs (eV)	Band gaps (eV)	Band gaps^{exp} (eV)
1d	0.316	1.56	2.40
2b	0.312	1.51	2.63
3a	0.166	1.97	3.10
3b	0.366	1.67	3.12

occurring in the ΓM_0 and ΓA subzones, corresponding, respectively, to the *bc* plane and *c* axis in the real space, and the dispersions are also corresponding to the maximal electron transfer integral directions. And in **2b** system, there are several directions with relative strong CB dispersions, particularly occurred in ΓV, VT and ΓU subzones, corresponding, respectively, to the *ab* and *ac* planes in the real space. With respect to system **3a**, the dispersion of the CB is small, indicating that the ability of **3a** in electron transport is limited. For the system **3b**, the largest CB dispersions occurring in BX, ΓZ and YE subzones, mainly corresponding to the *bc* plane and *c* axis in the real space, are also in agreement with the electron transfer integrals calculated in the hopping model. What's more, in accordance to the results based on hopping model, the systems **1d** and **3b** show 2-D electron transport behaviors, while the **2b** displays 3-D electron transport behaviors.

4. Conclusions

The electron injection ability, ambient stability and electron transport mobility are the most important factors affecting the performance of n-type transport materials. The present study systematically discussed the above factors based on the theoretical calculations and analysis on the FMO, ESP, EA, λ_{ele}, t_{ele}, μ_{ele} and band structures of 12 thiophene-based materials. The influence of fluorination, carbonylation and the conformation of the thiophene-core on the factors were investigated in depth.

With low LUMO energy level and high EA value, the material can easily trap an electron from the electrode or another monomer in the crystal. By introducing —F or (and) —CO substituents to a 4T-cored system, the LUMO energy level and the EA value are, respectively, lowered and heightened. And the effect of introducing —CO group is more significant than —F substitution. The ambient stability is indispensable for a transport material, especially for industrialization. And the weak oxidation stability of n-type transport material is a limitation for its development. What's more, by lowing FMO energies rendering the system less susceptible to oxidative degradation and the ambient stability will be enhanced. Introduction of fluorine substitutes and carbonyl groups will reduce the FMO energies, and the effect of carbonyl is more significant. Besides, when the substitutions introduce to a fused-ring thiophene-cored system, the energy lowing effect is more evident than the one of the chain-linked system, which means that for the fused-ring thiophene-cored systems, it is an excellent strategy to enhance the material's ambient stability by introducing fluorine substituentes and carbonyl groups.

For electron transport mobility (μ_{ele}), it is proved that introducing fluorine and carbonyl groups can lower the value of λ_{ele} to an extent. The fluorine end-substitutes have little effect on the LUMO delocalization degree, while introducing carbonyl group would cut off the conjugated chain. Investigating the distribution of ESP is an effective way to understand the electrostatic interaction in dimer. The fluorination and carbonylation, especially for the latter will affect the distribution ESPs, and introducing carbonyl group will form a negative charged center on the O atoms. This phenomenon might help to manipulate the packing manner.

Finally we supposed that the **3d** system should be a promising electron transporting material, because it exhibits the highest EA and small λ_{ele} with the lowest FMO energies ensuring a good ambient stability. From this we would like to predict the crystal structure of the **3d** system in the next and give a further study.

Acknowledgments

The authors gratefully acknowledge financial support from NSFC (21131001, 21273030, 21203019, 21203020 and 21363025), SRFDP and RGC ERG Joint Research Program (20120043140001) and the Science and Technology Development Planning of Jilin Province (201201071 and 201201067). We sincerely thank the Tobin J. Marks group of Northwestern University for offering the crystal file of **DF-4TA** (**3b**) system.

Appendix A. Supplementary data

Supplementary data associated with this article can be found, in the online version, at http://dx.doi.org/10.1016/j.jmgm.2015.04.001

References

[1] G. Horowitz, D. Fichou, X. Peng, Z. Xu, F. Garnier, A field-effect transistor based on conjugated alpha-sexithienyl, Solid State Commun. 72 (1989) 381–384.
[2] J. Burroughes, D. Bradley, A. Brown, R. Marks, K. Mackay, R. Friend, et al., Light-emitting diodes based on conjugated polymers, Nature 347 (1990) 539–541.
[3] J.R. Sheats, H. Antoniadis, M. Hueschen, W. Leonard, J. Miller, R. Moon, et al., Organic electroluminescent devices, Science 273 (1996) 884–888.
[4] C.D. Dimitrakopoulos, P.R. Malenfant, Organic thin film transistors for large area electronics, Adv. Mater. 14 (2002) 99–117.
[5] A. Facchetti, M. Mushrush, M.H. Yoon, G.R. Hutchison, M.A. Ratner, T.J. Marks, Building blocks for n-type molecular and polymeric electronics. Perfluoroalkyl- versus alkyl-functionalized oligothiophenes (*nT*; *n* = 2–6). Systematics of thin film microstructure, semiconductor performance, and modeling of majority charge injection in field-effect transistors, J. Am. Chem. Soc. 126 (2004) 13859–13874.
[6] A.R. Murphy, J.M. Frechet, Organic semiconducting oligomers for use in thin film transistors, Chem. Rev. 107 (2007) 1066–1096.
[7] Tan, M. Li, David Curtis, A.H. Francis, Characterization of organic p/n junction photodiodes based on poly (alkylthiophene)/perylene diimide bilayers, Chem. Mater. 15 (2003) 2272–2279.
[8] Congcheng Fan, Arjan P. Zoombelt, Hao Jiang, Weifei Fu, Jiake Wu, Wentao Yuan, Yong Wang, Hanying Li, Hongzheng Chen, Zhenan Bao, Solution-grown organic single-crystalline p-n junctions with ambipolar charge transport, Adv. Mater. 25 (2013) 5762–5766.
[9] A. Dodabalapur, H.E. Katz, L. Torsi, R.C. Haddon, Organic heterostructure field-effect transistors, Science 269 (1995) 1560–1562.
[10] Hagen Klauk, Ute Zschieschang, Jens Pflaum, Marcus Halik, Ultralow-power organic complementary circuits, Nature 445 (2007) 745–748.
[11] Hagen Klauk, Marcus Halik, Ute Zschieschang, Florian Eder, Dirk Rohde, Günter Schmid, Christine Dehm, Flexible organic complementary circuits, IEEE Trans. Electron Devices 52 (2005) 618–622.
[12] R. Capelli, F. Dinelli, S. Toffanin, F. Todescato, M. Murgia, M. Muccini, et al., Investigation of the optoelectronic properties of organic light-emitting transistors based on an intrinsically ambipolar material, J. Phys. Chem. C 112 (2008) 12993–12999.
[13] G.R. Dholakia, M. Meyyappan, A. Facchetti, T.J. Marks, Monolayer to multilayer nanostructural growth transition in N-type oligothiophenes on Au(111) and implications for organic field-effect transistor performance, Nano Lett. 6 (2006) 2447–2455.
[14] C. Shen, A. Kahn, J. Schwartz, Chemical and electrical properties of interfaces between magnesium and aluminum and tris-(8-hydroxy quinoline) aluminum, J. Appl. Phys. 89 (2001) 449–459.
[15] H. Katz, A. Lovinger, J. Johnson, C. Kloc, T. Siegrist, W. Li, et al., A soluble and air-stable organic semiconductor with high electron mobility, Nature 404 (2000) 478–481.
[16] D. De Leeuw, M. Simenon, A. Brown, R. Einerhand, Stability of n-type doped conducting polymers and consequences for polymeric microelectronic devices, Synth. Met. 87 (1997) 53–59.
[17] C.R. Newman, C.D. Frisbie, D.A. da Silva Filho, J.L. Brédas, P.C. Ewbank, K.R. Mann, Introduction to organic thin film transistors and design of n-channel organic semiconductors, Chem. Mater. 16 (2004) 4436–4451.
[18] B.A. Jones, A. Facchetti, M.R. Wasielewski, T.J. Marks, Tuning orbital energetics in arylene diimide semiconductors. Materials design for ambient stability of n-type charge transport, J. Am. Chem. Soc. 129 (2007) 15259–15278.
[19] V. Coropceanu, J. Cornil, D.A. da Silva Filho, Y. Olivier, R. Silbey, J.L. Brédas, Charge transport in organic semiconductors, Chem. Rev. 107 (2007) 926–952.
[20] Y.W. Park, Editorial for the conducting polymers for carbon electronics themed issue, Chem. Soc. Rev. 39 (2010) 2352–2353.
[21] M.H. Yoon, A. Facchetti, C.E. Stern, T.J. Marks, Fluorocarbon-modified organic semiconductors: molecular architecture, electronic, and crystal structure tuning of arene- versus fluoroarene-thiophene oligomer thin-film properties, Molecules 579 (2006) 2–801.
[22] T.J. Marks, n-Channel semiconductor materials design for organic complementary circuits, Acc. Chem. Res. 44 (2011) 501–510.
[23] L. Zhang, L. Tan, Z. Wang, W. Hu, D. Zhu, High-performance, stable organic field-effect transistors based on *trans*-1,2-(dithieno[2,3-b:3′,2′-d]thiophene)ethene, Chem. Mater. 21 (2009) 1993–1999.

[24] X.K. Chen, L.Y. Zou, S. Huang, C.G. Min, A.M. Ren, J.K. Feng, et al., Theoretical investigation of charge injection and transport properties of novel organic semiconductor materials—cyclic oligothiophenes, Org. Electron. 12 (2011) 1198–1210.
[25] Y. Geng, J.P. Wang, S.X. Wu, H.B. Li, F. Yu, G.C. Yang, et al., Theoretical discussions on electron transport properties of perylene bisimide derivatives with different molecular packings and intermolecular interactions, J. Mater. Chem. 21 (2011) 134–143.
[26] S.E. Koh, B. Delley, J.E. Medvedeva, A. Facchetti, A.J. Freeman, T.J. Marks, et al., Quantum chemical analysis of electronic structure and n- and p-type charge transport in perfluoroarene-modified oligothiophene semiconductors, J. Phys. Chem. B 110 (2006) 24361–24370.
[27] J.A. Letizia, A. Facchetti, C.L. Stern, M.A. Ratner, T.J. Marks, High electron mobility in solution-cast and vapor-deposited phenacyl-quaterthiophene-based field-effect transistors: toward N-type polythiophenes, J. Am. Chem. Soc. 127 (2005) 13476–13477.
[28] A. Facchetti, Y. Deng, A. Wang, Y. Koide, H. Sirringhaus, T.J. Marks, et al., Tuning the semiconducting properties of sexithiophene by,-substitution—,-diperfluorohexylsexithiophene: the first n-type sexithiophene for thin-film transistors, Angew. Chem. Int. Ed. 39 (2000) 4547–4551.
[29] T.J. Marks, A. Facchetti, H. Sirringhaus, H.R. Friend, WO PATENT 0 209 201, 2002.
[30] B.A. Facchetti, M. Mushrush, H.E. Katz, T.J. Marks, n-Type building blocks for organic electronics: a homologous family of fluorocarbon-substituted thiophene oligomers with high carrier mobility, Adv. Mater. 2 (2003) 33–38.
[31] A. Facchetti, M.H. Yoon, C.L. Stern, H.E. Katz, T.J. Marks, Building blocks for n-type organic electronics: regiochemically modulated inversion of majority carrier sign in perfluoroarene-modified polythiophene semiconductors, Angew. Chem. Int. Ed. 390 (2003) 0–3.
[32] C. Kim, P.Y. Huang, J.W. Jhuang, M.C. Chen, J.C. Ho, T.S. Hu, et al., Novel soluble pentacene and anthradithiophene derivatives for organic thin-film transistors, Org. Electron. 11 (2010) 1363–1375.
[33] J. Youn, P.Y. Huang, Y.W. Huang, M.C. Chen, Y.J. Lin, H. Huang, et al., Versatile α,ω-disubstituted tetrathienoacene semiconductors for high performance organic thin-film transistors, Adv. Funct. Mater. 4 (2012) 8–60.
[34] M.-H. Yoon, S.A. DiBenedetto, M.T. Russell, A. Facchetti, T.J. Marks, High-performance n-channel carbonyl-functionalized quaterthiophene semiconductors: thin-film transistor response and majority carrier type inversion via simple chemical protection/deprotection, Chem. Mater. 19 (2007) 4864–4881.
[35] X.D. Tang, Y. Liao, H.Z. Gao, Y. Geng, Z.M. Su, Theoretical study of the bridging effect on the charge carrier transport properties of cyclooctatetrathiophene and its derivatives, J. Mater. Chem. 22 (2012) 6907–6918.
[36] A.D. Becke, Density-functional exchange-energy approximation with correct asymptotic behavior, Phys. Rev. A: At. Mol. Opt. Phys. 38 (1988) 3098.
[37] C. Lee, Y. Wang, Quaternary stress changes in northern Taiwan and their tectonic significance, Geol. Soc. Chin. Proc. 31 (1988) 154–168.
[38] P. Stephens, F. Devlin, C. Chabalowski, M.J. Frisch, Ab initio calculation of vibrational absorption and circular dichroism spectra using density functional force fields, J. Phys. Chem. 98 (1994) 11623–11627.
[39] A.D. Becke, Density-functional thermochemistry. III. The role of exact exchange, J. Chem. Phys. 98 (1993) 5648–5652.
[40] J.P. Perdew, Density-functional approximation for the correlation energy of the inhomogeneous electron gas, Phys. Rev. B: Condens. Matter 33 (1986) 8822.
[41] P. Hariharan, J.A. Pople, Accuracy of AH n equilibrium geometries by single determinant molecular orbital theory, Mol. Phys. 27 (1974) 209–214.
[42] M.S. Gordon, The isomers of silacyclopropane, Chem. Phys. Lett. 76 (1980) 163–168.
[43] M.J. Frisch, J.A. Pople, J.S. Binkley, Self-consistent molecular orbital methods 25. Supplementary functions for Gaussian basis sets, J. Chem. Phys. 80 (1984) 3265–3269.
[44] P.C. Hariharan, J.A. Pople, The influence of polarization functions on molecular orbital hydrogenation energies, Theor. Chim. Acta 28 (1973) 213–222.
[45] M.M. Francl, W.J. Pietro, W.J. Hehre, J.S. Binkley, M.S. Gordon, D.J. DeFrees, et al., Self-consistent molecular orbital methods. XXIII. A polarization-type basis set for second-row elements, J. Chem. Phys. 77 (1982) 3654–3665.
[46] M.J. Frisch, G.W. Trucks, H.B. Schlegel, G.E. Scuseria, M.A. Robb, J.R. Cheeseman, et al., Gaussian 09. Revision A. 02., Gaussian, Inc, Wallingford, CT, 2009.
[47] J.E. Norton, J.L. Brédas, Polarization energies in oligoacene semiconductor crystals, J. Am. Chem. Soc. 130 (2008) 12377–12384.
[48] X.D. Tang, Y. Liao, H. Geng, Z.G. Shuai, Fascinating effect of dehydrogenation on the transport properties of N-heteropentacenes: transformation from p-to n-type semiconductor, J. Mater. Chem. 22 (2012) 18181–18191.
[49] S.I. Gorelsky, AOMix: Program for Molecular Orbital Analysis, University of Ottawa, US, 2007 http://www.sg-chem.net/
[50] X. Yang, L. Wang, C. Wang, W. Long, Z. Shuai, Influences of crystal structures and molecular sizes on the charge mobility of organic semiconductors: oligothiophenes, Chem. Mater. 20 (2008) 3205–3211.
[51] P.F. Barbara, T.J. Meyer, M.A. Ratner, Contemporary issues in electron transfer research, J. Phys. Chem. 100 (1996) 13148–13168.
[52] B.S. Brunschwig, J. Logan, M.D. Newton, N. Sutin, A semiclassical treatment of electron-exchange reactions. Application to the hexaaquoiron(II)–hexaaquoiron(III) system, J. Am. Chem. Soc. 102 (1980) 5798–5809.
[53] P. Siders, R. Marcus, Quantum effects for electron-transfer reactions in the inverted region, J. Am. Chem. Soc. 103 (1981) 748–752.
[54] M.D. Newton, N. Sutin, Electron transfer reactions in condensed phases, Annu. Rev. Phys. Chem. 35 (1984) 437–480.
[55] H. Gao, C. Qin, H. Zhang, S. Wu, Z.M. Su, Y. Wang, Theoretical characterization of a typical hole/exciton-blocking material bathocuproine and its analogues, J. Phys. Chem. A 112 (2008) 9097–9103.
[56] X.Y. Li, Electron transfer between tryptophan and tyrosine: theoretical calculation of electron transfer matrix element for intramolecular hole transfer, J. Comput. Chem. 22 (2001) 565–579.
[57] T. Fujita, H. Nakai, H. Nakatsuji, Abinitio molecular orbital model of scanning tunneling microscopy, J. Chem. Phys. 104 (1996) 2410–2417.
[58] E.F. Valeev, V. Coropceanu, D.A. da Silva Filho, S. Salman, J.L. Brédas, Effect of electronic polarization on charge-transport parameters in molecular organic semiconductors, J. Am. Chem. Soc. 128 (2006) 9882–9886.
[59] W.Q. Deng, W.A. Goddard, Predictions of hole mobilities in oligoacene organic semiconductors from quantum mechanical calculations, J. Phys. Chem. B 108 (2004) 8614–8621.
[60] L. Schein, A. McGhie, Band-hopping mobility transition in naphthalene and deuterated naphthalene, Phys. Rev. B: Condens. Matter 20 (1979) 1631–1639.
[61] G. Kresse, J. Furthmüller, Efficiency of ab-initio total energy calculations for metals and semiconductors using a plane-wave basis set, Comput. Mater. Sci. 6 (1996) 15–50.
[62] G. Kresse, J. Hafner, Ab initio molecular-dynamics simulation of the liquid-metal–amorphous-semiconductor transition in germanium, Phys. Rev. B: Condens. Matter 49 (1994) 14251.
[63] G. Kresse, J. Hafner, Ab initio molecular dynamics for liquid metals, Phys. Rev. B: Condens. Matter 47 (1993) 558.
[64] J. Perdew, Improved adsorption energetics within density functional theory using revised Perdew–Burke–Ernzerhof functionals, Phys. Rev. Lett. 77 (1996) 3865–3868.
[65] J.D. Pack, H.J. Monkhorst, Special points for brillouin-zone integrations—a reply, Phys. Rev. B: Condens. Matter 16 (1977) 1748.
[66] Q.X. Wu, Y. Geng, Y. Liao, X.-D. Tang, G.C. Yang, Z.M. Su, Theoretical studies of the effect of electron-withdrawing dicyanovinyl group on the electronic and charge-transport properties of fluorene–thiophene oligomers, Theor. Chem. Acc. 131 (2012) 1–9.
[67] A. Lv, S.R. Puniredd, J. Zhang, Z. Li, H. Zhu, W. Jiang, et al., High mobility, air stable, organic single crystal transistors of an n-type diperylene bisimide, Adv. Mater. 24 (2012) 2626–2630.
[68] P. Muller, Glossary of terms used in physical organic chemistry (IUPAC Recommendations 1994), Pure Appl. Chem. 66 (1994) 1077–1184.
[69] S.E. Koh, C. Risko, D.A. da Silva Filho, O. Kwon, A. Facchetti, J.L. Brédas, et al., Modeling electron and hole transport in fluoroarene-oligothiopene semiconductors: investigation of geometric and electronic structure properties, Adv. Funct. Mater. 18 (2008) 332–340.